buildings

MDPI

Article

Effect of Poly(ethylene glycol)–Poly(propylene glycol) Triblock Copolymers on Autogenous Shrinkage and Properties of Cement Pastes

Mohammad Sadegh Tale Masoule and Ali Ghahremaninezhad *

Department of Civil and Architectural Engineering, University of Miami, Coral Gables, FL 33146, USA
* Correspondence: a.ghahremani@miami.edu; Tel.: +1-305-284-3465

Abstract: This study investigates the hydration, microstructure, autogenous shrinkage, electrical resistivity, and mechanical properties of Portland cement pastes modified with PEG-PPG triblock copolymers with varied molecular weights. The early age properties including setting time and hydration heat were examined using the Vicat test and isothermal calorimetry. The hydration products and pore size distribution were analyzed using thermogravimetric analysis (TGA) and nitrogen adsorption, respectively. Mechanical properties and electrical resistivity were evaluated using the compressive strength test and electrochemical impedance spectroscopy (EIS). It was shown that the addition of the copolymers reduced the surface tension of the cement paste pore solution due to the presence of a hydrophobic block (PPG) in the molecular structure of the copolymers. The setting time and hydration heat were relatively similar in the control paste as well as the pastes modified with the copolymers. The results showed that copolymers were able to reduce the autogenous shrinkage in the paste due primarily to a reduction in pore solution surface tension. TGA showed a slight increase in the hydration degree of the paste modified with the copolymers. The compressive strength was reduced in the pastes modified with the copolymers that showed an increased volume of air voids. The addition of copolymers did not affect the electrical resistivity of the pastes except in the case where there was a large volume of air voids, which acted as electrical insulators.

Keywords: autogenous shrinkage; block copolymer; air-entraining; cement; admixture

check for updates

Citation: Masoule, M.S.T.; Ghahremaninezhad, A. Effect of Poly(ethylene glycol)–Poly(propylene glycol) Triblock Copolymers on Autogenous Shrinkage and Properties of Cement Pastes. *Buildings* **2024**, *14*, 283. https://doi.org/10.3390/buildings14010283

Academic Editor: Xiaoyong Wang

Received: 18 December 2023
Revised: 10 January 2024
Accepted: 18 January 2024
Published: 20 January 2024

Copyright: © 2024 by the authors. Licensee MDPI, Basel, Switzerland. This article is an open access article distributed under the terms and conditions of the Creative Commons Attribution (CC BY) license (https://creativecommons.org/licenses/by/4.0/).

1. Introduction

Air-entraining agents (AEAs) are an important class of concrete admixtures that increase the durability of concrete to repeated cycles of freeze-thaw [1]. They are generally surface-active agents with ionic/nonionic and hydrophobic sections and include natural and synthetic chemicals, including saponified rosin, alkyl ethoxylates, vinsol resins, and many other sulfonated hydrocarbons [1,2]. AEAs incorporate bubbles into concrete that turn into small, well-dispersed voids as the concrete hardens. Subsequently, these small voids relieve the pressure buildup of ice inside the concrete as it starts to freeze [3,4]. The surface activity of AEAs is therefore very influential on the incorporated bubbles and the characteristics of hardened concrete [1]. This is because the amount of incorporated bubbles and the stability of the bubble in fresh concrete depend on the interfacial properties that are governed by surface tension [1,5].

Concrete can experience different types of shrinkage during hydration, which include plastic and settlement shrinkage during its plastic stage, and chemical, autogenous, and drying shrinkage during its hardened state [6,7]. Chemical and autogenous shrinkage starts within hours of setting and can last for days and is mostly due to the consumption of water by hydration reactions within pores [7,8]. In chemical shrinkage, hydrating products consume water and create hydration products that occupy less space than the original products and cause an inward pressure [7,8]. Autogenous shrinkage starts when most of the water inside pores is consumed and only a thin layer of water remains on the pore surface.

The surface tension within this layer of water on the pores exerts a tensile force on the matrix that leads to autogenous shrinkage [7–9] and can cause both micro and macro cracks [8]. This effect is influenced by water/cement (W/C), pore size distribution, and moisture content [10] and can be a great concern with special types of concrete that have high binder content, including high-performance concrete [10,11]. Traditional approaches to mitigating shrinkage include quality control of raw materials, adjusting the mix proportions, the use of special low-heat cement, as well as incorporating chemical admixtures into the mixture [12]. Similar to AEAs, shrinkage-reducing admixtures (SRAs) are amphiphilic surface-active agents that adsorb on the air–water interface inside pores and reduce the surface tension of the adsorbed water layer [13].

Poly(ethylene glycol)–poly(propylene glycol) (PEG-PPG) triblock copolymers, also known as poloxamer or Pluronic®, are amphiphilic block polymers in the form of PPG-PEG-PPG or PEG-PPG-PEG [14]. The hydrophobic PPG and hydrophilic PEG blocks in these polymers give them good solubility, high surface tension reduction, and a range of net hydrophobicity (also known as the hydrophilic–lipophilic balance or HLB) [15]. These copolymers have seen prevalent use in different applications, such as foaming and emulsifying agents [16,17], drug delivery [18], and cosmetics [19]. They have also been used in biomedical cement including brushite foams [20].

Due to the surface activity and molecular structure of PEG-PPG triblock copolymers, they can be suitable candidates for both AEA and SRA. However, the effect of these copolymers on cementitious materials has not been investigated in the past. In a previous study by our group, the air-entraining characteristics of these copolymers and their effect on the microstructure of hardened cement paste were investigated [21]. The novelty of this paper is to investigate the effect of PEG-PPG copolymers with varied molecular weights on the properties of Portland cement paste, including autogenous shrinkage, setting time and hydration, compressive strength, electrical resistivity, and pore microstructure.

2. Materials and Methods

2.1. Materials and Sample Preparation

Four copolymers with different molecular weights were purchased from Millipore-Sigma (Burlington, MA, USA) and used without modification. These copolymers are listed in Table 1. In this paper, the term copolymer is synonymous with PEG-PPG triblock copolymers. A type I/II Portland cement from Cemex (Miami cement plant, Miami, FL, USA) was obtained and used for cement paste preparation. The oxide composition of the cement, as reported by the manufacturer, is given in Table 2. Cement paste was prepared by mixing cement, deionized water (DI), and copolymers in fixed concentration, and the mixture proportions are reported in Table 3. The copolymers, in the concentration of 0.25% *w*/*w*% cement, were added to DI and mixed until fully dissolved. Cement was then added to a bucket containing the copolymer solutions and mixed for 70 s at high speed, with a 10 s pause after the first 30 s of mixing to scrape paste from the interior wall of the bucket. The paste was poured into 12 in × 1 in prism molds, vibrated for 30 s, and then wrapped in plastic foil. After 24 h, the prisms were demolded, sealed in double plastic bags, and left to cure for 28 days. The hardened cement paste samples are denoted with a CEM-, followed by the name of the copolymer. All the samples were prepared at a W/C of 0.5, except for autogenous shrinkage and surface tension experiments, which were made at a W/C of 0.3 and 2, respectively.

Table 1. Chemical structure of the PEG-PPG triblock copolymers used in this study. The first 3 copolymers are in the form of PEG-PPG-PEG, whereas the last one—COP3300—has a reversed order of blocks, in the form of PPG-PEG-PPG.

Designation	Pluronic® Identifier	Molecular Structure	Molecular Weight (Da)	HLB
COP1100	L-31	$[PEG]_a$ $[PPG]_b$ $[PEG]_a$ *	1100	5
COP8400	F-68 LF	$[PEG]_a$ $[PPG]_b$ $[PEG]_a$	8400	29
COP14600	F-108	$[PEG]_a$ $[PPG]_b$ $[PEG]_a$	14,600	27
COP3300	31R1	$[PPG]_a$ $[PEG]_b$ $[PPG]_a$	3300	1

* a and b are the number of units in each block.

Table 2. Oxide composition of type I/II cement.

Composition	(%)
CaO	64
SiO_2	20.6
Na_2O	0.1
K_2O	0.3
Al_2O_3	4.8
Fe_2O_3	3.5
MgO	0.9
SO_3	3.4
LOI	2.4

Table 3. Mixture proportions of cement pastes modified with copolymers.

Sample	Cement (g)	W/C	Copolymer (*w*/*w*% Cement)
Ctrl	1000	0.5	0
CEM-COP1100	1000	0.5	0.25% COP1100
CEM-COP8400	1000	0.5	0.25% COP8400
CEM-COP14600	1000	0.5	0.25% COP14600
CEM-COP3300	1000	0.5	0.25% COP3300

2.2. Methods

A series of experiments have been performed to understand the full extent of the effect of PEG-PPG block copolymers on fresh and hardened cement paste. The list of these experiments and the relevant standards are summarized in Table 4.

Table 4. Summary of the experiments.

Experiment	Relevant Standard
Surface tension of pore solution	-
Autogenous shrinkage	ASTM C1698-19
FTIR	-
Isothermal calorimetry	ASTM C1679-17
Thermogravimetry analysis	ASTM C1872-18
Setting time	ASTM C191-21
Pore size characterization using nitrogen adsorption	ISO 15901-2
Compressive strength	ASTM C109-C109M-21
Electrical impedance spectroscopy	ASTM C1876-19

2.2.1. Surface Tension of Pore Solution Containing Copolymers

The surface tension of the pore solution extracted from fresh cement paste containing different copolymers was measured to study how the copolymers affect the surface tension of the pore solution in cementitious materials. Solutions of copolymer with a concentration of 0.25% *w*/*w*% cement were prepared and mixed for 1 min with cement at a W/C of 2.

The paste was then left to rest for 20 min, after which it was transferred to 50 mL tubes and centrifuged at a rate of 4400 rpm for 5 min. The separated clear pore solution at the top of the tube was then pipetted into a syringe and was passed through a VWR 0.22 µm RC (regenerated cellulose membranes) syringe filter to remove any particles left. The surface tension of the gathered pore solution was subsequently measured with a BZY 201 tensiometer (MXBaoheng, Hangzhou, China) using the platinum plate method with 3–4 repetitions.

2.2.2. Autogenous Shrinkage

The methodology of ASTM C1698-19 was adopted to measure the effect of copolymers on the autogenous shrinkage of cement paste. The fresh cement paste samples were cast into corrugated polyethylene tubes (length: 42 cm, diameter: 2.9 cm) according to the standard and capped. The change in the length of the tubes was measured in 12 h increments for the first week and every day after that for up to 28 days at an ambient temperature of 22 °C. The length measurement was conducted using a digital displacement gauge (Germann Instruments, Evanston, IL, USA). Figure 1 shows the corrugated tubes used to measure the autogenous shrinkage.

Figure 1. Corrugated tubes filled with fresh paste, used to measure the autogenous shrinkage.

2.2.3. Fourier-Transform Infrared Spectroscopy (FTIR)

PerkinElmer Frontier spectrometer (PerkinElmer, Shelton, CT, USA) was used to find the FTIR transmittance spectrum of copolymers in their solid or liquid form directly. The transmittance was measured for 3 repetitions in the range of 600–4000 cm^{-1} wavelength, with a resolution of 2 cm^{-1} and 16 accumulations. The background air signal was collected and subtracted from the copolymer spectrum.

2.2.4. Isothermal Calorimetry (IC)

A TAM Air 8-channel calorimeter (TA Instruments, Lindon, UT, USA) was used to study the effect of copolymer addition on the hydration heat release of the cement paste. The pastes were prepared in a smaller batch according to the sample preparation methodology described before, but the mixing was performed by hand. Approximately 7 g of paste was poured into a glass ampule and studied at 23 °C for up to 90 h.

2.2.5. Thermogravimetry Analysis (TGA)

To prepare the samples for the thermogravimetric analysis, core samples were extracted from the center of 1-inch cubes, ground in a mortar and pestle, and passed through the #200 sieve to only retain sizes below 75 µm. The powders were then dried at 40 °C in a vacuum oven for 24 h before testing. The experiment was performed on a DTG-60H (Shimadzu, Tampa, FL, USA) using nitrogen gas as the atmosphere with a flow rate of 50 mL/min. The temperature range was from 25 to 1000 °C with a temperature ramp of 20 °C/min and a hold time of 5 min at the peak. The differential thermal analysis (DTA) curve was calculated based on the mass loss curve. The $Ca(OH)_2$ (CH) content was quantified in the range of 450–530 °C, and the $CaCO_3$ (CC) content was quantified in the range of 725–760 °C [22–26].

2.2.6. Setting Time

Setting times were determined with the Vicat needle equipment, and measurements were performed at 10 min increments at 5 discrete locations on the paste until a lack of impression on the paste was observed, indicating final setting times, respectively. Figure 2 shows the pastes prior to the setting time experiment.

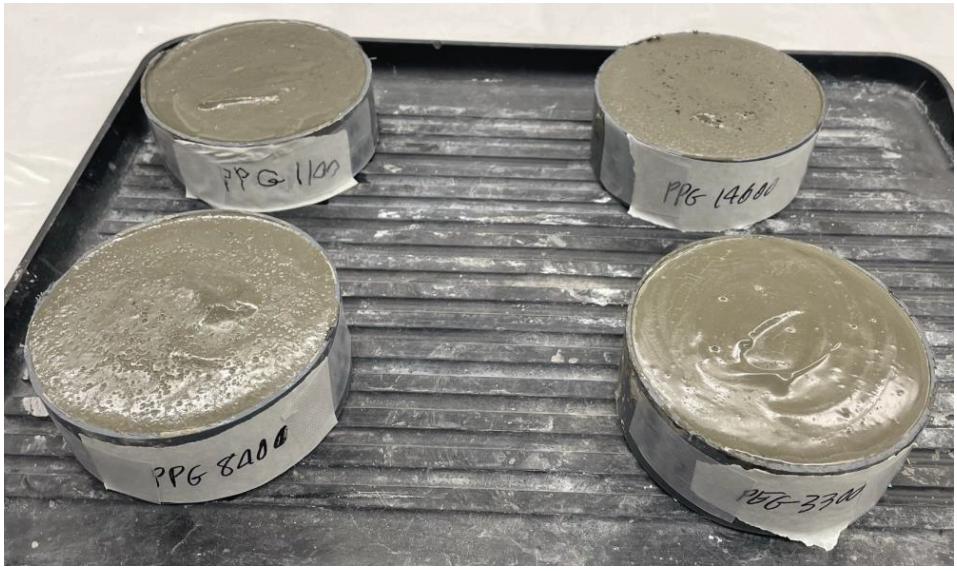

Figure 2. Pastes used to measure the setting time of cement pastes modified with copolymer.

2.2.7. Pore Size Characterization Using Nitrogen Adsorption

Pore size analysis was performed with a Nova 600 Physiosorption instrument (Anton Paar, Houston, TX, USA). Ground powders were prepared similarly to the TGA experiment and degassed at 105 °C for 3 h. The samples were then submerged in liquid nitrogen and the full adsorption–desorption isotherms were measured. The pore size distribution analysis was performed using the software (Kaomi for Nova) provided by the manufacturer.

2.2.8. Compressive Strength

The compressive strength of the 1-inch cube samples was measured using a SATEC instrument (SATEC, Union, NJ, USA). Five repetitions of each series were tested at 28 days of curing and the average was reported.

2.2.9. Electrical Impedance Spectroscopy (EIS)

The electrical resistivity of the 1-inch samples was determined at 28 days using a Reference 600 Potentiostat (Gamry, Warminster, PA, USA). Two pieces of foam were immersed in a 2 molar NaCl solution and placed in the interface between the metal plate electrodes

and the cement sample to lower the influence of interface contact. The measurements were performed at a frequency range of 106–10 Hz and at a voltage of 250 mV.

3. Results and Discussion

3.1. FTIR

Figure 3 displays the FTIR transmittance spectrum for the copolymers in their native form. Since no water solvent was used, the O–H peaks at 3300 cm^{-1} and 1640 cm^{-1} that are associated with water are not present. Major peaks corresponding to C–H backbone groups at 2970 cm^{-1} for PPG and 2860 cm^{-1} for PEG are observed [27]. Another major peak is observed at 1090 cm^{-1} that belongs to C–O in-plane stretching groups between PEG and PPG [28].

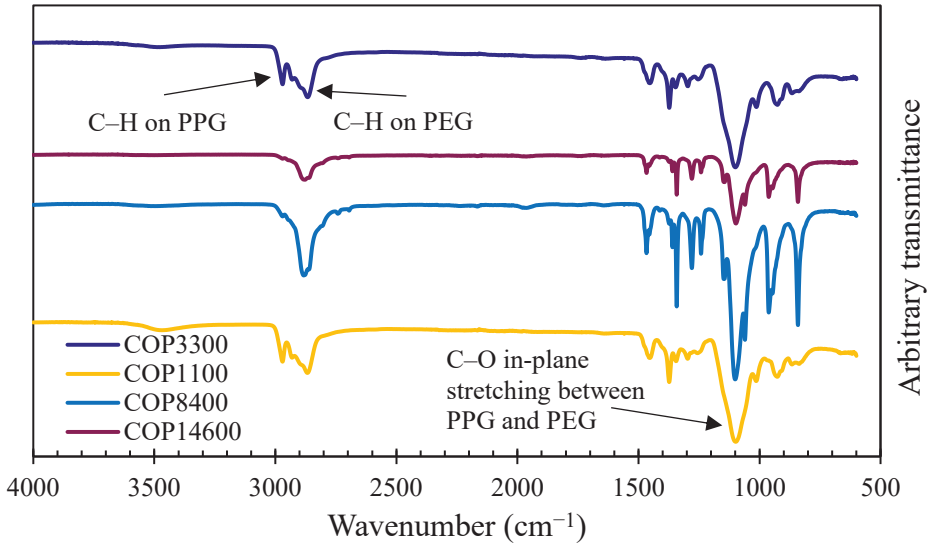

Figure 3. FTIR curve of copolymers in their native form.

3.2. Surface Tension of Pore Solution

Figure 4 displays the surface tension of the pore solution extracted from control paste and pastes containing copolymer at a concentration of 0.25% *w*/*w*% cement. The surface tension of the pore solution of control at around 71 mN/m does not show any changes compared to the surface tension of deionized water. On the other hand, the pore solution of the pastes modified with copolymers has noticeably reduced surface tension, averaging around 45 mN/m.

Surface tension is an important parameter that governs many of the interfacial interactions in cementitious materials and affects the microstructure [1]. The behavior of different chemicals such as AEAs and SRA is affected by their surface tension. The molecular properties of the surfactant, including the length and size of the hydrophobic groups, molecular size, and charge can affect the surface tension of the surfactant [1,5]. In copolymers, a lower PEG/PPG value or a smaller HLB generally indicates higher hydrophobicity and lower surface tension [15]. COP3300 has the lowest surface tension among all the copolymers, which is due to the very hydrophobic nature of COP3300. The exceptionally low HLB of 1 in COP3300, displayed in Table 1, is an indication of the high hydrophobicity of COP3300. Although the other copolymers have higher hydrophilicity, the presence of hydrophobic PPG groups in their structure keeps their surface tension relatively low.

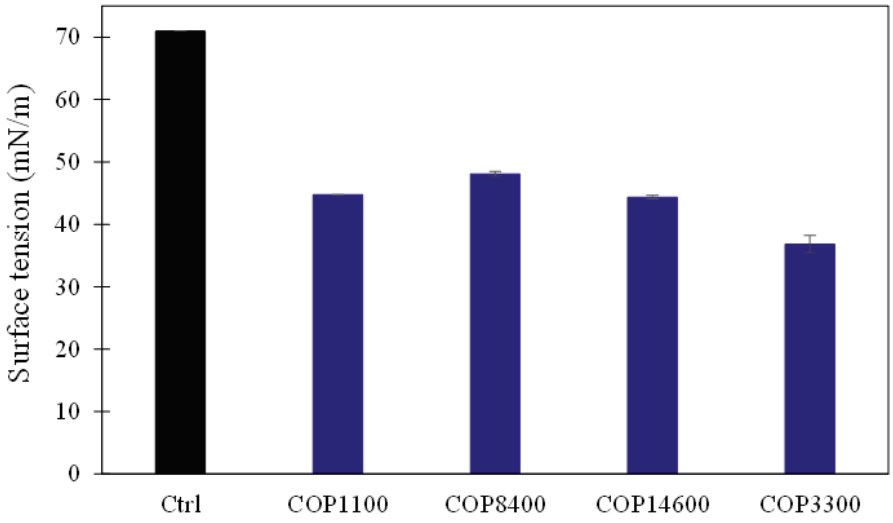

Figure 4. Surface tension of the pore solution extracted from fresh cement paste.

3.3. Setting Time

The setting times of the control paste and the pastes with copolymers are shown in Figure 5. It is seen that the setting time of CEM-COP14600 is the highest compared to other pastes at both W/C of 0.3 and 0.5. CEM-COP8400 showed a slightly larger setting time compared to the control paste and CEM-COP1100 and CEM-COP3300 at W/C of 0.3. It has been shown in the literature that the addition of charged polymers could affect setting time in cement pastes due to the adsorption of charged polymers on the heterogeneous phases of hydrating cement particles, which could decrease the dissolution rate and delay the hydration reaction and the setting time [29,30]. Since the copolymers used in our study are non-ionic and do not adsorb onto cement particles, their effect on cement hydration and solid skeleton formation is small. However, in CEM-COP14600, due to the presence of a large volume of air voids that reduce the volume fraction of the hydrating cement in the paste, the setting time is slightly delayed as shown in Figure 5 for this paste.

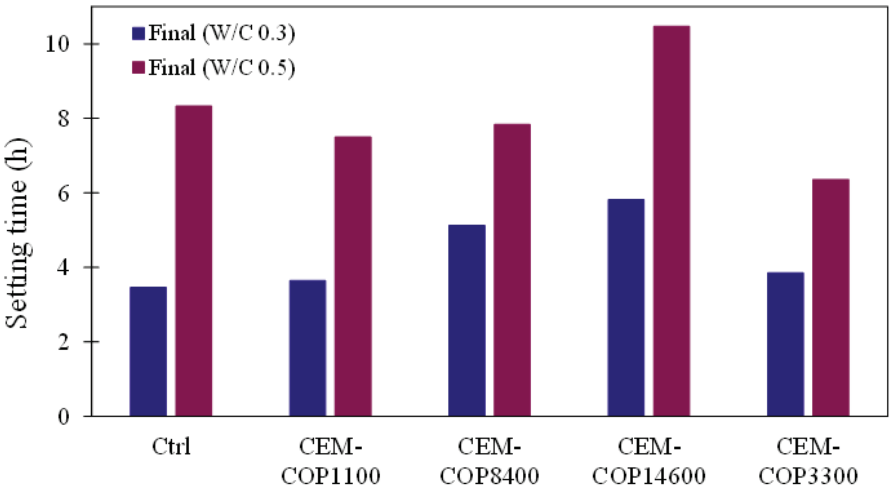

Figure 5. The final setting time of the pastes, at two W/C of 0.3 and 0.5.

3.4. Isothermal Calorimetry

The rate of hydration heat and cumulative heat of the control paste, and the pastes modified with the copolymers are shown in Figure 6. It is seen in Figure 6a that all pastes showed a peak at about the same time. This peak corresponds to the formation of binding

phases produced by the hydration reaction [31]. This peak is typically associated with the final setting time of the pastes. It is evident that the heat rate results are generally in good agreement with the setting time results discussed earlier. Another peak marked in the heat rate curves shown in Figure 6a is also seen in all pastes, which corresponds to the secondary ettringite formation [31]. A slight increase in the magnitude of the peak in the pastes modified with copolymers compared to the control paste is noticed. The cumulative heat curves of the pastes show a relatively similar behavior. It appears that the cumulative heat of the pastes with the copolymers was slightly higher compared to that of the control paste at late times of hydration. The results show a low impact of copolymers on the hydration mechanisms of cement pastes. One influential parameter can be traced back to the low adsorption of copolymers on the cement surface since many polymers need to adsorb on the surface before interfering with the hydration mechanisms [32]. The slight increase in the hydration of the pastes with the copolymers could be due to higher homogenous nucleation of cement due to lower interfacial energy stemming from the surface activity of surfactants as suggested by Gueit et al. [33].

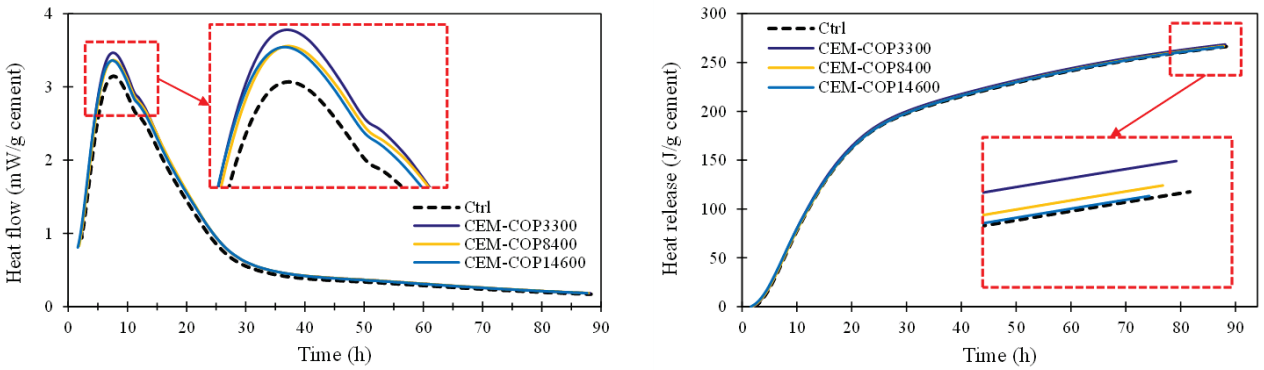

Figure 6. (**a**) Rate of heat evolution and (**b**) cumulative heat release of the pastes.

3.5. Pore Size Distribution

Figure 7a shows the pore size distribution of the paste microstructure, with an inset graph breaking down the total pore volume per gram of cement into two categories: 4–10 nm and 10–50 nm. In Figure 7b, the cumulative pore volume of the pastes modified with copolymer is shown. It is evident from Figure 7a,b that the addition of copolymers increased the peak amplitude of very fine pores around 4–6 nm for almost all copolymers. However, this increase in peak amplitude does not necessarily correspond to a higher capillary pore volume for the entire size range. Specifically, CEM-COP8400 exhibited a much sharper and narrower peak at 5 nm compared to the control, but the total pore size remained unchanged in both small and larger pore categories. Similarly, CEM-COP14600 did not show significant changes compared to the control. On the other hand, CEM-COP3300 showed a 45% increase in total pore volume, where a substantial portion of it was situated in the 4–10 nm range. Depending on the size, charge, and structure of the side chains, polymers can have a significant impact on the capillary porosity. In a study by Tian et al. [34], a noticeable difference in the specific surface area of cement pastes modified with different polycarboxylate polymers was observed. On the other hand, PEG-PPG copolymers display minimal adsorption to cement particles [21] and minimal impact on hydration properties as discussed previously. This can be traced back to the block copolymers' lack of charge and smaller molecular size. Although nitrogen absorption is a viable method of measuring small capillary pores, it is not descriptive of the entire capillary range in cement paste since it only measures the pores in a small range of less than 50–100 nm.

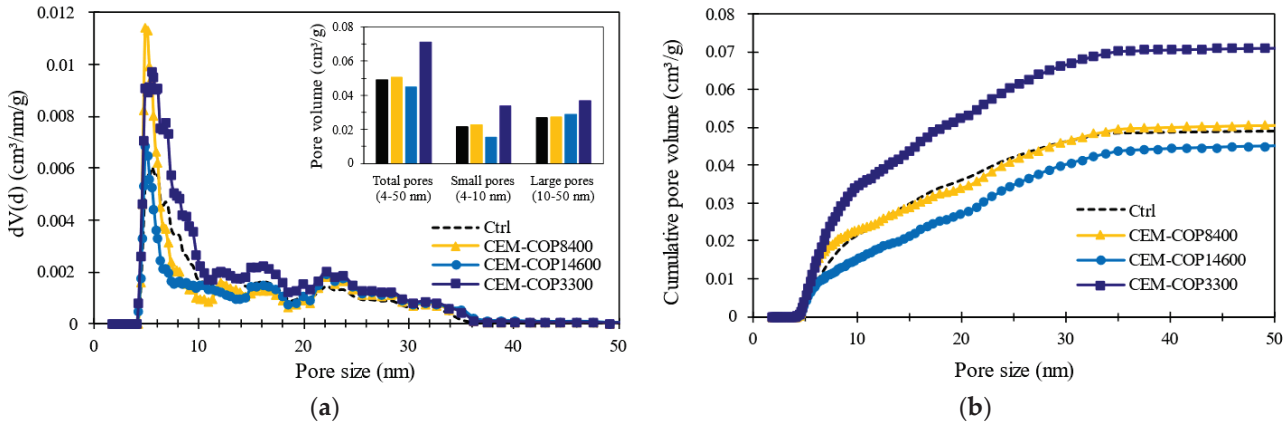

Figure 7. (**a**) Pore size distribution and (**b**) cumulative pore volume of the pastes.

3.6. Autogenous Shrinkage

The autogenous shrinkage of the control paste and the pastes modified with copolymers is shown in Figure 8. It is seen that the paste with the copolymers had a lower autogenous shrinkage compared to the control paste. The autogenous shrinkage increased more rapidly in all pastes in the first 3 days and then continued to increase at a smaller rate as seen in the figure. In cement pastes with a low W/C, water is consumed as a hydration reaction occurs leading to self-desiccation. With a reduction in the relative humidity, the stress is developed in the capillary pore solution, which pulls on the solid skeleton of the paste, and this manifests as an overall reduction in the volume of the material [10]. This reduction in volume occurs without interactions with the external environment and is called autogenous shrinkage. In a constrained condition, autogenous shrinkage leads to the buildup of tensile stress in the solid skeleton, which could result in crack formation when the critical tensile strength is reached. The capillary stress in the pore solution is dependent on the surface tension of the pore solution. Thus, the reduction in the surface tension of the pore solution could reduce autogenous shrinkage in the paste [35,36]. A comparison of the surface tension results shown in Figure 4 and the autogenous shrinkage results indicates that the reduction in the autogenous shrinkage of the paste with the copolymers is primarily due to the effect of copolymers in reducing the surface tension of the pore solution in the pastes. It should be noted that the presence of air voids reduces the volume fraction of the capillary pores that are responsible for autogenous shrinkage; thus, it is expected that the lower volume fraction of capillary pores in CEM-COP14600 with a large air-void porosity could contribute to a lower autogenous shrinkage in this paste, compared to other pastes as seen in Figure 7.

Besides surface tension, some studies argue that autogenous shrinkage is affected predominantly by the pore volume below 50 nm [37,38], where a higher pore volume would induce higher drying stress and therefore more shrinkage. Such a relationship was not observed for the copolymer samples of the current study. Control and CEM-COP14600 show similar pore volumes in the pore range of below 50 nm, and CEM-COP3300 has a higher pore volume than the other pastes. But in terms of shrinkage, all copolymers show lower shrinkage than control. Thus, the amount of change in pore solution surface tension seems to have a greater effect, compared to the effect of changes in pore volume on the autogenous shrinkage of the pastes examined in this study.

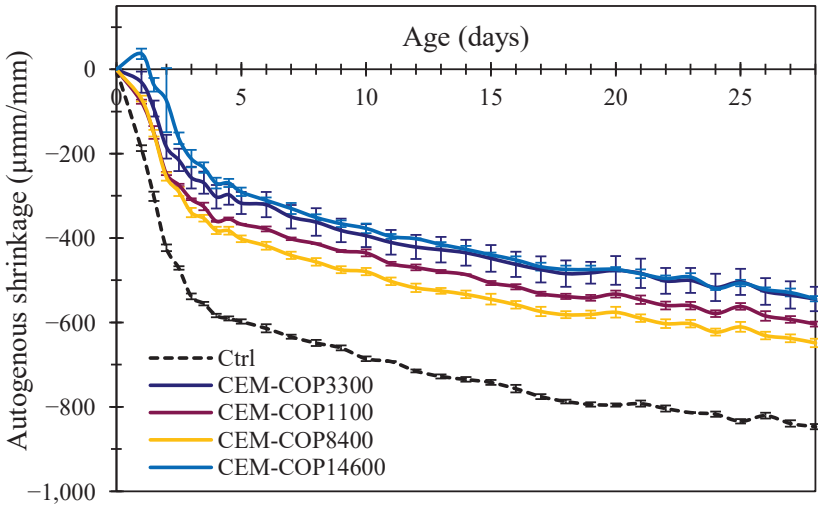

Figure 8. Autogenous shrinkage of the pastes.

3.7. TGA

Figure 9 shows the TGA and DTA curves for the control and pastes containing a 0.25% concentration of copolymers at 28 days of curing. The quantification of the CH and CC phases in this paste is reported in Table 5. The results show a slight increase in the amount of CH content for the pastes modified with copolymers compared to the control, which can suggest a slightly higher degree of hydration in the modified pastes. This is because an increase in the amount of hydration phases usually points to an increase in the degree of hydration of the cement paste, especially since there are no CH-consuming reactions in the paste. Previous studies have shown that highly ionic surfactants can affect the CH content, often lowering the CH amount by forming salts with Ca^{2+} [39] or by altering the dissolution and precipitation of phases of cement [40–42]. In contrast, nonionic surfactants have fewer interactions with cement due to the lack of charge and low adsorption [43]. Despite this, a small increase in CH content is observed in the TGA results. This observation seems to be in agreement with a slight increase in cumulative heat of hydration in the pastes modified with the copolymers compared to the control paste, as discussed in Figure 6. Gueit et al. [33] suggested that this increase is the result of a higher homogenous nucleation of cement due to a lower interfacial energy stemming from the surface activity of surfactants. Contrary to CH, there do not seem to be any significant changes in the CC content of the pastes.

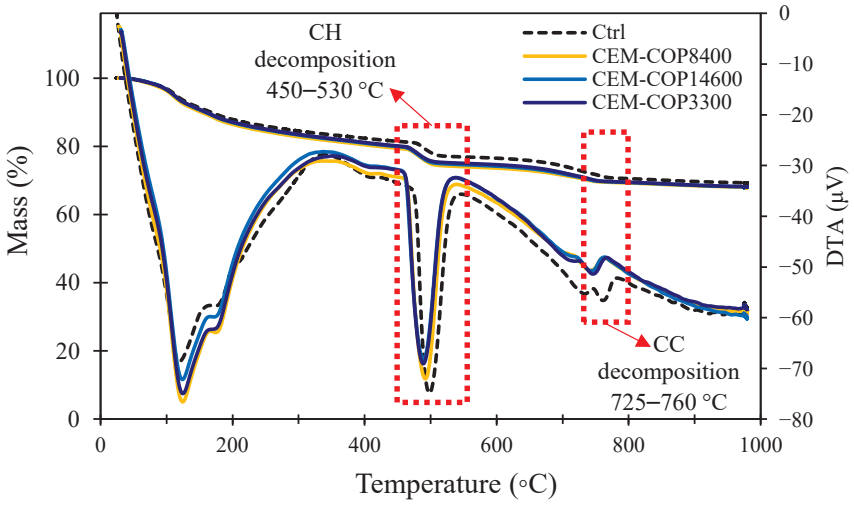

Figure 9. TGA and DTA curves of the pastes.

Table 5. CH and CC content of the paste obtained from TGA.

Sample	CH (%)	CC (%)
Ctrl	18.09	2.93
CEM-COP8400	21.62	2.70
CEM-COP14600	21.01	2.88
CEM-COP3300	20.27	3.24

3.8. Compressive Strength

Figure 10a displays the compressive strength of the control paste and pastes modified with 0.25% copolymer at 28 days of curing. It is seen that CEM-COP3300 and CEM-COP1100 do not show noticeable change compared to the control paste, but CEM-COP8400 and CEM-COP14600 had 17.8% and 39.6% reductions in compressive strength, respectively. The compressive strength is correlated with the dry density of the hardened pastes at 28 days, and this relationship is displayed in Figure 10b. It follows that as the amount of stable foam increases inside the fresh paste, the macro air-void porosity of the hardened paste increases accordingly as air bubbles turn into voids [44]. This higher porosity reduces the dry density of hardened cement paste, which respectively leads to lower compressive strength [45]. The relationship between dry density and compressive strength is well-established in the literature [45,46]. The dry density of the hardened pastes is also presented in Table 6. CEM-COP3300 and CEM-COP1100 showed a small decrease in dry density, and this did not seem to affect their compressive strength compared to the control paste. In contrast, density reduces in CEM-COP8400, and more noticeably in CEM-COP14600, and as such, this contributes to the decreased compressive strength of these two pastes relative to the control paste.

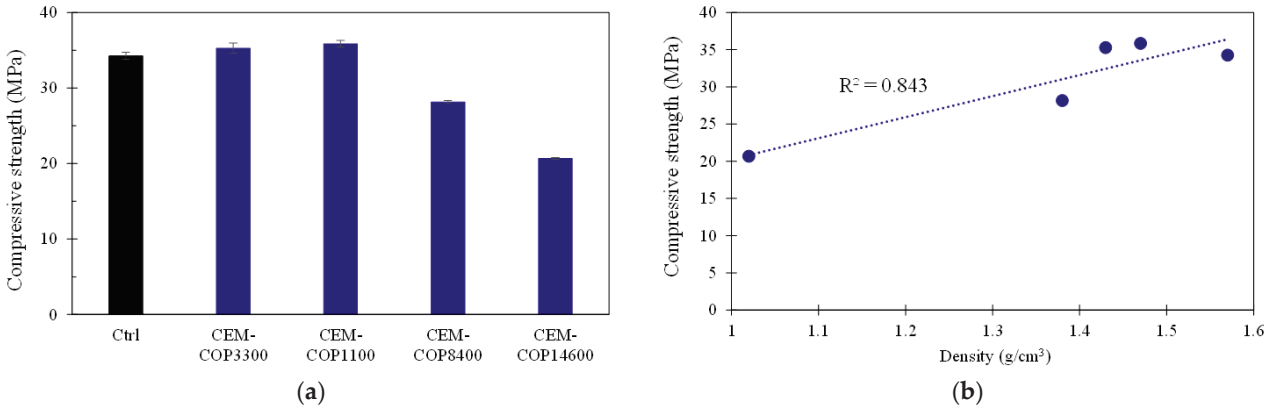

Figure 10. Compressive strength of the control paste and the pastes with copolymers. (**a**) Compressive strength of samples. (**b**) Relationship between compressive strength and density.

Table 6. Dry density of the pastes.

Paste	Dry Density (g/cm^3)
Ctrl	1.57
CEM-COP3300	1.43
CEM-COP1100	1.47
CEM-COP8400	1.38
CEM-COP14600	1.02

3.9. Electrical Resistivity

Figure 11 displays the electrical resistivity of the control paste and pastes modified with copolymers at 28 days of hydration. The pore structure and resistivity of the pore solution

are the main factors governing the electrical resistivity of cementitious materials [47–57]. Except for CEM-COP14600, no significant difference in electrical resistivity between the control paste and the pastes modified with copolymers was observed. CEM-COP14600 showed a 21% increase in electrical resistivity compared to the control paste. As discussed earlier, CEM-COP14600 and CEM-COP8400 had an air-void volume fraction of 31.17% and 3.23%, respectively [21]. The effect of air voids on the electrical resistivity depends on the degree of saturation of the air voids. If filled with fluid, they act as electrical conductors decreasing the total electrical resistivity of the paste. Conversely, if completely empty, the air voids act as electrical insulators increasing the electrical resistivity of the paste [58]. Since the air voids in the pastes studied here are expected to have very low water content, they are expected to behave like an insulator. Thus, this explains the noticeable higher electrical resistivity of CEM-COP14600 compared to other pastes. In the case of CEM-COP8400, the effect of a small volume fraction of air voids might have been countered by a small increase in the capillary porosity or the change in the pore solution resistivity resulting in an insignificant change in the electrical resistivity of CEM-COP8400 compared to the control paste.

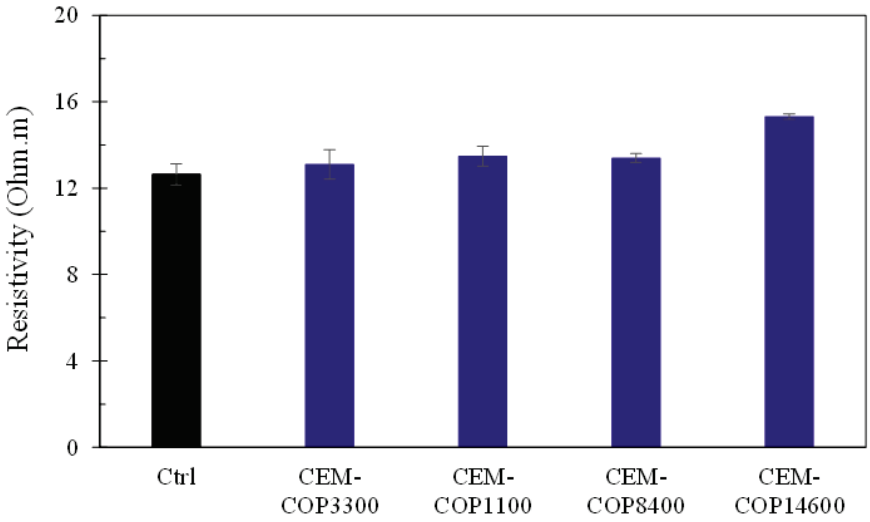

Figure 11. Electrical resistivity of the control paste and the pastes with copolymers.

4. Conclusions

In this study, the hydration, autogenous shrinkage, microstructure, electrical resistivity, and compressive strength of cement pastes modified with PEG-PPG block copolymers with different molecular structures were studied. The following conclusions are drawn:

- Copolymers effectively reduced the surface tension of pore solution due to the presence of hydrophobic blocks in their molecular structure.
- In terms of hydration, they did not have a significant effect on hydration kinetics or setting time of cement paste. This is mostly due to the low interactions between cement particles and copolymers, resulting from the nonionic nature of these copolymers.
- The autogenous shrinkage was reduced in the paste modified with copolymers compared to the control paste. The reduction in pore solution surface tension and subsequently capillary pressure is responsible for reduced autogenous shrinkage in the pastes modified with the copolymers.
- TGA analysis showed a small increase in the $Ca(OH)_2$ content at 28 days of curing in the pastes modified with the copolymers compared to the control paste indicating a small enhancement in hydration in the modified pastes.
- Compressive strength was lower in the pastes modified with the copolymers that had a higher air-void volume fraction. In the pastes modified with copolymers that

did not have increased air voids, the compressive strength was similar to that of the control paste.

- The electrical resistivity of the pastes with the copolymers was similar to that of the control paste except in the case of CEM-COP14600, where a noticeable increase in electrical resistivity was observed. The presence of a large volume of air voids that act as electrical insulators is responsible for the higher electrical resistivity in this paste.

Author Contributions: Conceptualization, M.S.T.M. and A.G.; methodology, M.S.T.M.; software, M.S.T.M.; validation, M.S.T.M. and A.G.; formal analysis, M.S.T.M.; investigation, M.S.T.M. and A.G.; resources, A.G.; data curation, M.S.T.M. and A.G.; writing—original draft preparation, M.S.T.M. and A.G.; writing—review and editing, M.S.T.M. and A.G.; visualization, M.S.T.M.; supervision, A.G.; project administration, A.G.; funding acquisition, A.G. All authors have read and agreed to the published version of the manuscript.

Funding: This study was performed at the Advanced Infrastructure Materials Research Laboratory at the University of Miami and was supported by the National Science Foundation under the CAREER award number 1846984 and the MRI award number 1920127. Any opinions, findings, and conclusions or recommendations expressed in this material are those of the authors and do not necessarily reflect the views of the National Science Foundation.

Data Availability Statement: The raw data supporting the conclusions of this article will be made available by the authors on request.

Conflicts of Interest: The authors declare no conflicts of interest.

References

1. Tunstall, L.E.; Ley, M.T.; Scherer, G.W. Air entraining admixtures: Mechanisms, evaluations, and interactions. *Cem. Concr. Res.* **2021**, *150*, 106557. [CrossRef]
2. Zhao, H.; Yang, Y.; Shu, X.; Qiao, M.; Dong, L.; Ran, Q. Understanding the adsorption of air entraining agents on portlandite: A combined DFT and molecular dynamics investigation. *Appl. Surf. Sci.* **2023**, *627*, 157341. [CrossRef]
3. Powers, T. A Working Hypothesis for Further Studies of Frost Resistance of Concrete, Concrete.Org (1945). Available online: https://www.concrete.org/publications/internationalconcreteabstractsportal.aspx?m=details&i=8684&m=details&i=8684 (accessed on 1 January 2024).
4. Powers, T.C.; Willis, T.F. The Air Requirement of Frost Resistant Concrete. In Proceedings of the Twenty-Ninth Annual Meeting of the Highway Research Board, Washington, DC, USA, 13–16 December 1949; Volume 29.
5. Masoule, M.S.T.; Baffoe, E.; Ghahremaninezhad, A. On the physicochemical properties and foaming characteristics of proteins in cement environment. *Constr. Build. Mater.* **2023**, *366*, 130204. [CrossRef]
6. Synthesis of Rapid Setting Repair Materials Final Report February 2022 Sponsored by Federal Highway Administration Technology Transfer Concrete Consortium (TTCC) Pooled Fund TPF-5(313) (Part of Intrans Project 15-532). Available online: https://intrans.iastate.edu/ (accessed on 7 December 2023).
7. Burris, L.E.; Alapati, P.; Kurtis, K.E.; Hajibabaee, A.; Ley, M.T. Understanding Shrinkage in Alternative Binder Systems. Special Publication 336; In *Symposium Paper*; American Concrete Institute: Indianapolis, IN, USA, 2019; pp. 73–90. [CrossRef]
8. Lura, P.; Jensen, O.M.; van Breugel, K. Autogenous shrinkage in high-performance cement paste: An evaluation of basic mechanisms. *Cem. Concr. Res.* **2003**, *33*, 223–232. [CrossRef]
9. Bentz, D.; Jensen, O. Mitigation strategies for autogenous shrinkage cracking. *Cem. Concr. Compos.* **2004**, *26*, 677–685. [CrossRef]
10. Wu, L.; Farzadnia, N.; Shi, C.; Zhang, Z.; Wang, H. Autogenous shrinkage of high performance concrete: A review. *Constr. Build. Mater.* **2017**, *149*, 62–75. [CrossRef]
11. Mousavinezhad, S.; Gonzales, G.J.; Toledo, W.K.; Garcia, J.M.; Newtson, C.M.; Allena, S. A Comprehensive Study on Non-Proprietary Ultra-High-Performance Concrete Containing Supplementary Cementitious Materials. *Materials* **2023**, *16*, 2622. [CrossRef]
12. Liu, J.; Tian, Q.; Wang, Y.; Li, H.; Xu, W. Evaluation Method and Mitigation Strategies for Shrinkage Cracking of Modern Concrete. *Engineering* **2021**, *7*, 348–357. [CrossRef]
13. Zhan, P.-M.; He, Z.-H. Application of shrinkage reducing admixture in concrete: A review. *Constr. Build. Mater.* **2019**, *201*, 676–690. [CrossRef]
14. Pitto-Barry, A.; Barry, N.P.E. Pluronic®block-copolymers in medicine: From chemical and biological versatility to rationalisation and clinical advances. *Polym. Chem.* **2014**, *5*, 3291–3297. [CrossRef]
15. Alexandridis, P.; Hatton, T.A. Poly(ethylene oxide)-poly(propylene oxide)-poly(ethylene oxide) block copolymer surfactants in aqueous solutions and at interfaces: Thermodynamics, structure, dynamics, and modeling. *Colloids Surf. A Physicochem. Eng. Asp.* **1995**, *96*, 1–46. [CrossRef]

16. Kabong, M.A.; Focke, W.W.; Du Toit, E.L.; Rolfes, H.; Ramjee, S. Breakdown mechanisms of oil-in-water emulsions stabilised with Pluronic F127 and co-surfactants. *Colloids Surf. A Physicochem. Eng. Asp.* **2020**, *585*, 124101. [CrossRef]
17. del Castillo-Santaella, T.; Yang, Y.; Martínez-González, I.; Gálvez-Ruiz, M.J.; Cabrerizo-Vílchez, M.; Holgado-Terriza, J.A.; Selles-Galiana, F.; Maldonado-Valderrama, J. Effect of Hyaluronic Acid and Pluronic-F68 on the Surface Properties of Foam as a Delivery System for Polidocanol in Sclerotherapy. *Pharmaceutics* **2020**, *12*, 1039. [CrossRef]
18. Kabanov, A.V.; Batrakova, E.V.; Alakhov, V.Y. Pluronic®block copolymers as novel polymer therapeutics for drug and gene delivery. *J. Control. Release* **2002**, *82*, 189–212. [CrossRef]
19. Yoon, K.-S.; Yang, S.J. Preparation and Evaluation of Pluronic Lecithin Organogels in Cosmetics. *J. Cosmet. Sci.* **2021**, *72*, 325–346. Available online: https://www.researchgate.net/publication/353374215 (accessed on 14 December 2023).
20. Unosson, J.; Montufar, E.B.; Engqvist, H.; Ginebra, M.; Persson, C. Brushite foams—The effect of Tween®80 and Pluronic®F-127 on foam porosity and mechanical properties. *J. Biomed. Mater. Res. Part B Appl. Biomater.* **2016**, *104*, 67–77. [CrossRef]
21. Masoule, M.S.T.; Ghahremaninezhad, A. The Relationship between Molecular Structure and Air-Entraining of Poly(Ethylene Glycol)-Poly(Propylene Glycol) Triblock Surfactants in Cementitious Materials (Under review).
22. Snoeck, D.; Van Tittelboom, K.; Steuperaert, S.; Dubruel, P.; De Belie, N. Self-healing cementitious materials by the combination of microfibres and superabsorbent polymers. *J. Intell. Mater. Syst. Struct.* **2014**, *25*, 13–24. [CrossRef]
23. Wang, J.; Snoeck, D.; Van Vlierberghe, S.; Verstraete, W.; De Belie, N. Application of hydrogel encapsulated carbonate precipitating bacteria for approaching a realistic self-healing in concrete. *Constr. Build. Mater.* **2014**, *68*, 110–119. [CrossRef]
24. Kim, T.; Olek, J. Effects of Sample Preparation and Interpretation of Thermogravimetric Curves on Calcium Hydroxide in Hydrated Pastes and Mortars. *Transp. Res. Rec. J. Transp. Res. Board* **2012**, *2290*, 10–18. [CrossRef]
25. Ashraf, W.; Olek, J. Carbonation activated binders from pure calcium silicates: Reaction kinetics and performance controlling factors. *Cem. Concr. Compos.* **2018**, *93*, 85–98. [CrossRef]
26. Mignon, A.; Snoeck, D.; Schaubroeck, D.; Luickx, N.; Dubruel, P.; Van Vlierberghe, S.; De Belie, N. pH-responsive superabsorbent polymers: A pathway to self-healing of mortar. *React. Funct. Polym.* **2015**, *93*, 68–76. [CrossRef]
27. Dmitrenko, M.; Penkova, A.; Atta, R.; Zolotarev, A.; Plisko, T.; Mazur, A.; Solovyev, N.; Ermakov, S. The development and study of novel membrane materials based on polyphenylene isophthalamide—Pluronic F127 composite. *Mater. Des.* **2019**, *165*, 107596. [CrossRef]
28. Elmowafy, M.; Alruwaili, N.K.; Shalaby, K.; Alharbi, K.S.; Altowayan, W.M.; Ahmad, N.; Zafar, A.; Elkomy, M. Long-Acting Paliperidone Parenteral Formulations Based on Polycaprolactone Nanoparticles; the Influence of Stabilizer and Chitosan on In Vitro Release, Protein Adsorption, and Cytotoxicity. *Pharmaceutics* **2020**, *12*, 160. [CrossRef] [PubMed]
29. Jansen, D.; Goetz-Neunhoeffer, F.; Neubauer, J.; Haerzschel, R.; Hergeth, W.-D. Effect of polymers on cement hydration: A case study using substituted PDADMA. *Cem. Concr. Compos.* **2013**, *35*, 71–77. [CrossRef]
30. Su, Z.; Bijen, J.; Larbi, J. Influence of polymer modification on the hydration of portland cement. *Cem. Concr. Res.* **1991**, *21*, 535–544. [CrossRef]
31. Baral, A.; Roesler, J.R. Hydration and Air Entrainment Challenges of High-Volume Fly Ash Concrete Pavement. In Proceedings of the 12th International Conference on Concrete Pavements, Online, 27 September–1 October 2022; pp. 298–305. [CrossRef]
32. Lange, A.; Plank, J. Contribution of non-adsorbing polymers to cement dispersion. *Cem. Concr. Res.* **2016**, *79*, 131–136. [CrossRef]
33. Gueit, E.; Darque-Ceretti, E.; Tintillier, P.; Horgnies, M. Surfactant-induced growth of a calcium hydroxide coating at the concrete surface. *J. Coatings Technol. Res.* **2012**, *9*, 337–346. [CrossRef]
34. Tian, H.; Kong, X.; Cui, Y.; Wang, Q.; Wang, D. Effects of polycarboxylate superplasticizers on fluidity and early hydration in sulfoaluminate cement system. *Constr. Build. Mater.* **2019**, *228*, 116711. [CrossRef]
35. Lopes, A.N.M.; Silva, E.F.; Molin, D.C.C.D.; Filho, R.D.T. Shrinkage-reducing admixture: Effects on durability of high-strength concrete. *ACI Mater. J.* **2013**, *110*, 365–374.
36. Rajabipour, F.; Sant, G.; Weiss, J. Interactions between shrinkage reducing admixtures (SRA) and cement paste's pore solution. *Cem. Concr. Res.* **2008**, *38*, 606–615. [CrossRef]
37. Ding, D.; Zhang, L.; Zhao, J.; Li, C.; Wang, Z. Effects of air-entraining agent and polypropylene fiber on the mechanical properties, autogenous shrinkage, and fracture properties of fully recycled aggregate concrete. *Front. Mater.* **2022**, *9*, 633. [CrossRef]
38. Wang, Z.; Li, G. A prediction model for autogenous shrinkage of high-performance concrete in bridge engineering. *Mag. Concr. Res.* **2013**, *65*, 1325–1335. [CrossRef]
39. Betioli, A.; Filho, J.H.; Cincotto, M.; Gleize, P.; Pileggi, R. Chemical interaction between EVA and Portland cement hydration at early-age. *Constr. Build. Mater.* **2009**, *23*, 3332–3336. [CrossRef]
40. Uchikawa, H.; Hanehara, S.; Shirasaka, T.; Sawaki, D. Effect of admixture on hydration of cement, adsorptive behavior of admixture and fluidity and setting of fresh cement paste. *Cem. Concr. Res.* **1992**, *22*, 1115–1129. [CrossRef]
41. Kamali, M.; Ghahremaninezhad, A. Effect of Biomolecules on the Nanostructure and Nanomechanical Property of Calcium-Silicate-Hydrate. *Sci. Rep.* **2018**, *8*, 9491. [CrossRef] [PubMed]
42. Kamali, M.; Ghahremaninezhad, A. A Study of Calcium-Silicate-Hydrate/Polymer Nanocomposites Fabricated Using the Layer-By-Layer Method. *Materials* **2018**, *11*, 527. [CrossRef]
43. Feneuil, B.; Pitois, O.; Roussel, N. Effect of surfactants on the yield stress of cement paste. *Cem. Concr. Res.* **2017**, *100*, 32–39. [CrossRef]

44. Guo, T.; Qiao, M.; Shu, X.; Dong, L.; Shan, G.; Liu, X.; Guo, Y.; Ran, Q. Characteristic analysis of air bubbles on the rheological properties of cement mortar. *Constr. Build. Mater.* **2022**, *316*, 125812. [CrossRef]
45. Othman, R.; Jaya, R.P.; Muthusamy, K.; Sulaiman, M.; Duraisamy, Y.; Abdullah, M.M.A.B.; Przybył, A.; Sochacki, W.; Skrzypczak, T.; Vizureanu, P.; et al. Relation between Density and Compressive Strength of Foamed Concrete. *Materials* **2021**, *14*, 2967. [CrossRef]
46. Falliano, D.; De Domenico, D.; Ricciardi, G.; Gugliandolo, E. Experimental investigation on the compressive strength of foamed concrete: Effect of curing conditions, cement type, foaming agent and dry density. *Constr. Build. Mater.* **2018**, *165*, 735–749. [CrossRef]
47. Bu, Y.; Weiss, J. The influence of alkali content on the electrical resistivity and transport properties of cementitious materials. *Cem. Concr. Compos.* **2014**, *51*, 49–58. [CrossRef]
48. Jain, J.; Neithalath, N. Electrical impedance analysis based quantification of microstructural changes in concretes due to non-steady state chloride migration. *Mater. Chem. Phys.* **2011**, *129*, 569–579. [CrossRef]
49. Farzanian, K.; Vafaei, B.; Ghahremaninezhad, A. The Behavior of Superabsorbent Polymers (SAPs) in Cement Mixtures with Glass Powders as Supplementary Cementitious Materials. *Materials* **2019**, *12*, 3597. [CrossRef]
50. Vafaei, B.; Farzanian, K.; Ghahremaninezhad, A. Effect of Hydrogels Containing Nanosilica on the Properties of Cement Pastes. *J. Compos. Sci.* **2021**, *5*, 105. [CrossRef]
51. Prabahar, J.; Vafaei, B.; Baffoe, E.; Ghahremaninezhad, A. The Effect of Biochar on the Properties of Alkali-Activated Slag Pastes. *Constr. Mater.* **2022**, *2*, 1–14. [CrossRef]
52. Rajabipour, F.; Sant, G.; Weiss, J. Development of electrical conductivity-based sensors for health monitoring of concrete materials. In Proceedings of the TRB Annual Conference, Washington, DC, USA, 21–25 January 2007; p. 16.
53. Neithalath, N.; Jain, J. Relating rapid chloride transport parameters of concretes to microstructural features extracted from electrical impedance. *Cem. Concr. Res.* **2010**, *40*, 1041–1051. [CrossRef]
54. Schwarz, N.; DuBois, M.; Neithalath, N. Electrical conductivity based characterization of plain and coarse glass powder modified cement pastes. *Cem. Concr. Compos.* **2007**, *29*, 656–666. [CrossRef]
55. Farnam, Y.; Todak, H.; Spragg, R.; Weiss, J. Electrical response of mortar with different degrees of saturation and deicing salt solutions during freezing and thawing. *Cem. Concr. Compos.* **2015**, *59*, 49–59. [CrossRef]
56. Neithalath, N.; Weiss, J.; Olek, J. Characterizing Enhanced Porosity Concrete using electrical impedance to predict acoustic and hydraulic performance. *Cem. Concr. Res.* **2006**, *36*, 2074–2085. [CrossRef]
57. Neithalath, N.; Persun, J.; Hossain, A. Hydration in high-performance cementitious systems containing vitreous calcium aluminosilicate or silica fume. *Cem. Concr. Res.* **2009**, *39*, 473–481. [CrossRef]
58. Wong, H.; Pappas, A.; Zimmerman, R.; Buenfeld, N. Effect of entrained air voids on the microstructure and mass transport properties of concrete. *Cem. Concr. Res.* **2011**, *41*, 1067–1077. [CrossRef]

Disclaimer/Publisher's Note: The statements, opinions and data contained in all publications are solely those of the individual author(s) and contributor(s) and not of MDPI and/or the editor(s). MDPI and/or the editor(s) disclaim responsibility for any injury to people or property resulting from any ideas, methods, instructions or products referred to in the content.